International Journal of Nanomedicine

Dovepress
Taylor & Francis Group

Open Access Full Text Article

ORIGINAL RESEARCH

Delivery of Polypeptide Drugs Using Nanoparticles Made of Recombinant Spider Silks Derived From MaSp4 Protein

Zheng Peng, Rui Wen

Department of Radiation Oncology, The Quzhou Affiliated Hospital of Wenzhou Medical University, Quzhou People's Hospital, Quzhou, Zhejiang, 324002, People's Republic of China

Correspondence: Zheng Peng; Rui Wen, Email hdpz@163.com; wenr@ucas.ac.cn

Background: Spider silk protein is a biocompatible and biodegradable protein that can self-assemble into various morphological materials for biomedical applications including drug delivery carriers. Spiders can spin up to seven types of silk fibers, each containing multiple silk proteins. Despite the numerous potential applications of these silk proteins, comprehensive and in-depth research on their specific roles and efficacy in drug delivery has yet to be conducted. The authors designed three new bioengineered spider silk proteins (M4R2, M4R4, and M4R6) and examined its property as a carrier of polypeptided drugs.

Materials and Methods: To obtain the M4R2, M4R4, and M4R6 proteins, three constructs comprising 2, 4, and 6 repeat units of Araneus ventricosus major ampullate spidroin 4 (MaSp4) were engineered for prokaryotic expression using the *Escherichia coli* expression system. The particles made of M4R2, M4R4, and M4R6 silks were produced using a high concentration of potassium phosphate buffer. The physical properties of these particles were characterized by scanning electron microscopy (SEM) and zeta potential analysis. The cytotoxicity of particles was analyzed using MTT assay. The loading and release profiles of drugs were examined spectrophotometrically.

Results: The three bioengineered silk proteins, M4R2, M4R4, and M4R6, were constructed, produced, and purified. These proteins exhibit self-assembly properties and formed particles. Furthermore, the these particles were not cytotoxic and had similar particle sizes but differed in loading efficiency and drug release rate. The loading of drugs into the M4R2 particles was more efficient (>95%) than that into the M4R4 and M4R6 particles. In addition, the continuous release of ChMAP-28 from M4R2 particles over 30 days indicates its potential as a sustained-release carrier for positively charged peptide drugs. The high stability, excellent loading efficiency, and sustained-release performance of M4R2 particles make them an ideal choice for the delivery of positively charged peptide drugs.

Conclusion: We developed three recombinant silk proteins, M4R2, M4R4, and M4R6, demonstrating that M4R2 particles, with stable colloidal properties, high loading efficiency of positively charged drugs, and controlled release rates, are promising new particulate drug carrier systems for the delivery of polypeptided drugs.

Keywords: spider silk, particles, drug delivery, polypeptided drugs

Introduction

Owing to their outstanding delivery efficiency and controllability, various biodegradable polymers have been fabricated as nanoparticles for drug delivery systems (DDS).[1–3] Nanoparticles and microspheres have been extensively employed to achieve controlled-release delivery of multiple therapeutic agents such as peptides and proteins. Because these pharmaceutical ingredients are prone to protease degradation, chemical modification, and denaturation or aggregation during storage, special formulation designs are indispensable to safeguard their stability and activity.[4] Therefore, an ideal particulate drug delivery system must have a variety of characteristics, including biodegradability, no toxicity, controlled drug release, easy processability, and low cost.[5,6] Among these materials, polylactic-co-glycolic acid (PLGA) has received much biomedical attention and is the most extensively studied drug carrier owing to its biodegradability and low cost.[7,8] However, the utilization of organic solvents and the creation of an acidic microenvironment during the

Received: 12 December 2024
Accepted: 26 February 2025
Published: 3 March 2025

Graphical Abstract

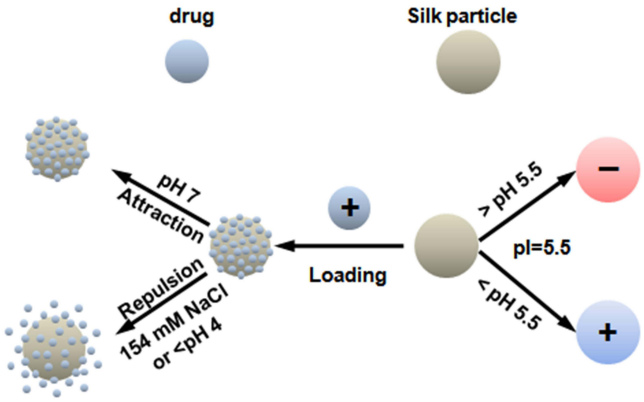

preparation process render PLGA unsuitable as a carrier for protein drug delivery.[9,10] As PLGA degrades within the body, it releases lactic acid and glycolic acid, which can accumulate inside the carrier and lead to a decrease in pH. This acidic environment may adversely affect both the stability of the encapsulated drug and the surrounding cellular milieu. Therefore, a series of protein-based biomaterials are urgently needed to overcome the aforementioned limitations that have hindered the progress and development of the drug delivery field.

Protein-based biomaterials for drug delivery have garnered significant attention due to their biocompatibility, biodegradability, and versatility in encapsulating and releasing therapeutic agents, such as zein (from corn), soy proteins, and silk fibroin (from silkworms and spiders).[11,12] Among these animal and plant-derived proteins, silk fibers from *Bombyx mori* and spiders are promising candidates for delivery systems because of their biocompatibility, biodegradability, and noncytotoxic properties.[13] Compared to silkworm silk, spider silk demonstrates greater strength, higher extensibility, and lower natural yield. Owing to the rapid development of spider silk protein production and purification, a large variety of spider silk proteins with different molecular weights has been produced under laboratory conditions and can be processed into various types of materials, including hydrogels, fibers, nanoparticles, and capsules.[14,15] Moreover, multiple bioengineered spider silk proteins (spidroins) have been explored for drug delivery applications, demonstrating that spidroin-based particles are stable, nontoxic, highly efficient, and easy processability.[16–18] Most of the reported spidroin-based particles used as DDS are fabricated based on two major ampullate spidroins (MaSp1 and MaSp2), which are components of spider dragline silk.[19,20] However, previous studies have indicated that dragline silk is composed of more than two spidroins with distinct amino acid composition and physical properties.[21,22] Recently, a novel major ampullate spidroin (MaSp4) was identified, which possesses unique repeat motifs compared to MaSp1 and MaSp2.[23] MaSp4 contains GPGPQ motifs that form β-turn structures, but it lacks the poly-alanine motifs characteristic of MaSp1 and MaSp2. Given the uniqueness of this sequence, it is necessary to further explore the applications of MaSp4 as a drug carrier.

In this study, we designed and fabricated three bioengineered spidroins, M4R2, M4R4, and M4R6, based on the core domain of MaSp4 from *Araneus ventricosus*. M4R2, M4R4, and M4R6 were composed of two, four, and six repetitive units of the MaSp4 consensus motif, respectively.

The colloidal stability of particles based on these recombinant spidroins was studied at varying pH, ionic strength, and long-term storage. To investigate the feasibility of loading silk particles with functional peptides, the antitumor peptide ChMAP-28, which exhibits a positive net charge, was selected as a model peptide. We examine the loading and release behaviors of ChMAP-28 under varying ionic strength and pH conditions of the release buffer. Fluorescein isothiocyanate (FTIC)-labeled MaSp4 particles were used for subsequent analysis of the corresponding particle dispersions by fluorescence microscopy. The antitumor activity of ChMAP-28 loaded MaSp4 particles was analyzed using flow cytometry.

Materials and Methods

Production of the Recombinant Spidroins M4R2, M4R4, and M4R6

All three recombinant spidroins contained amino acid sequences from the natural core sequence of *A. ventricosus* MaSp4. M4R2, M4R4, and M4R6 contained two, four, and six repeat units of MaSp4, respectively, and their sequences are presented in Figure 1A. The molecular weights of M4R2, M4R4, and M4R6 are 11.2, 22.4, 33.6 kDa, respectively. Since the isoelectric point of these three proteins is 5.5, they have an overall negative charge (physiological condition) at pH 7.4.

To obtain recombinant proteins, these three recombinant spidroin genes were synthesized by Beijing Tsingke Biotech Co., Ltd., ligated into the pEHS expression vector, and transformed into *E. coli* BL21 cells. Gene expression was induced at OD_{600} = 0.8 using 0.1 mm IPTG followed by further 20 h of shake culture in LB medium containing 50 μg/mL ampicillin at 20°C. Following induction, the cells were harvested by centrifugation, suspended in lysis buffer (20 mm Tris-HCl, 300 mm NaCl, pH 8.0), and lysed using a Pressure Cell Press JN-3000 Plus (JNBIO, China). The samples were then centrifuged to remove insoluble materials. For protein purification, the supernatant was combined with a Ni-NTA column and gently rocked at 4°C for 1h, then the resin was washed three times with wash buffer (20 mm Tris-HCl, 300 mm NaCl, 20 mm imidazole, pH 8.0), followed by elution with elution buffer (20 mm Tris-HCl, 300 mm NaCl, 250 mm imidazole, pH 8.0). Finally, the purified samples were lysed in lysis buffer at 4°C overnight and then analyzed using SDS-PAGE. The silk protein concentration was calculated by measuring the absorbance by UV spectroscopy at 280 nm. The peptide ChMAP-28 was synthesized by Beijing Tsingke Biotech Co. Ltd.

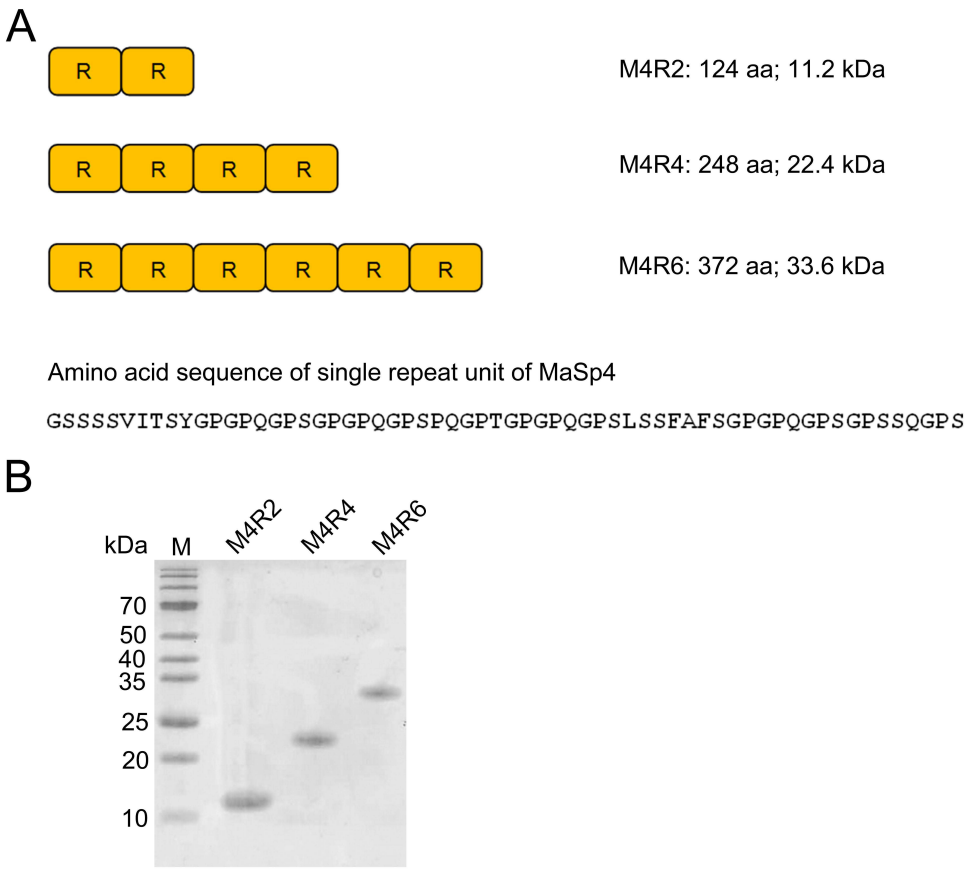

Figure 1 Analysis of M4R2, M4R4, and M4R6 proteins. (**A**) Schematic illustration and amino acid sequences of M4R2, M4R4, and M4R6 proteins. The molecular weight and the number of amino acid residues of each recombinant spidroin are shown. (**B**) SDS-PAGE analysis of purified recombinant proteins, followed by visualization via Coomassie Brilliant Blue staining.

https://doi.org/10.2147/IJN.S510273

Preparation of M4R2, M4R4, and M4R6 Particles

Three recombinant MaSp4 solutions (c = 1.5 mg/mL) were dialyzed against 2 M potassium phosphate (pH 8.0) at room temperature, using a regenerated cellulose membrane. After dialysis, the particles were collected by centrifugation and washed thrice with ultrapure water. Subsequently, the obtained particle dispersions were sonicated for 15 minutes. The particle concentrations were determined gravimetrically.

Dynamic Light Scattering (DLS) and Zeta-Potential Analysis

Dynamic light scattering and zeta potential measurements were performed using a Zetasizer Nano ZS instrument (Malvern Instruments). For DLS, the samples were diluted to a concentration of 0.01 mg/mL in the corresponding buffer before analysis of the Z-average values of the particles. The zeta potential of the particles was also determined at the same concentration and temperature as those used for particle size analysis. In addition, the width of the particle size distribution expressed by the polydispersity index (PI) was also determined using a Zetasizer Nano ZS instrument (Malvern Instruments). All measurements were performed in triplicates.

Scanning Electron Microscopy (SEM)

The particle suspension was placed on a slip and dried. Next, the samples were coated with gold alloy in a Pelco SC-7 autosputter coater with a thickness monitor. Particle morphology was observed using a Hitachi SU8010 instrument at an accelerating voltage of 3 kV. The SEM experiments were conducted at 25°C and 55% humidity.

Colloidal Stability of M4R2, M4R4, and M4R6 Particles

To investigate the colloidal stability of the particles under tumor microenvironment conditions (characterized by low pH and ionic strength) and physiological conditions, the stability was examined at pH values of 6, 6.5, and 7, and at different ionic strengths of 50 mm, 100 mm, and 154 mm NaCl. After the centrifugation of the stock dispersion, the particle concentration was adjusted to 0.2 mg/mL. Subsequently, the samples were analyzed to determine the particle size and zeta potential using a Zetasizer Nano ZS, as described in the above sections. Furthermore, storage stability of the three particle dispersions in ultrapure water was investigated at 4°C over a period of 3 months.

Cytotoxicity Study

Cytotoxicity was determined by measuring cell viability using the MTT assay. NIH 3T3 fibroblasts (ATCC, Manassas, USA) were grown in DMEM supplemented with 10% fetal bovine serum and 80 μg/mL gentamycin. Next, the cells were seeded at 1×10^4/well in 96-well plate and cultured at 37°C for 24 h. After incubation, the particle suspensions were added to the cell cultures at different concentrations and incubated for an additional 72 h. Subsequently, 50 μL of the MTT reagent was added to each well and incubated for 4 h. After removing the medium, insoluble purple formazan was dissolved in 200 μL DMSO. The absorbance of each cell line was measured at 570 nm using a microplate reader (BioTek Instruments, USA). The experiments were performed in triplicate. Cells without particles were used as negative controls.

Loading of Particles With ChMAP-28

ChMAP-28 was loaded in 10 mm phosphate buffer (pH 7.0) with different ionic strengths (50, 100, and 154 mm NaCl). Spider silk particles were collected from the stock dispersion via centrifugation and redispersed in different phosphate buffers before loading. Lyophilized ChMAP-28 was dissolved in an identical buffer solution to prepare a ChMAP-28 stock solution. The obtained particle suspension and ChMAP-28 stock solution were mixed at room temperature to achieve a final silk particle concentration of 0.5 mg/mL and the desired w/w-ratio (%) of ChMAP-28 to silk particles. After 1 h of incubation, the samples were used for DLS measurements, and the supernatant obtained by centrifugation was analyzed for residual protein content using a BCA Protein Assay Kit. The encapsulation efficiency and loading were calculated using Equations (1) and (2), respectively.

$$\text{Loading efficiency}\,(\%) = \frac{\text{ChMAP}-28 \text{ loaded on silk particles}\,(\mu\,\text{g})}{\text{ChMAP}-28 \text{ initially added}\,(\mu\,g)} \times 100 \quad (1)$$

$$\text{Loading}\,(\%) = \frac{\text{ChMAP} - 28 \text{ loaded on silk particles}\,(\mu\,\text{g})}{\text{silk particles}\,(\mu\,g)} \times 100 \quad (2)$$

In vitro Release Studies of ChMAP-28 From Silk Particles

In order To investigate the effects of pH and ionic strength on the release of ChMAP-28, all release experiments were performed with a payload of 15% ChMAP-28 and a silk particle concentration of 1 mg/mL at 37°C. In vitro release studies were performed under physiological (pH 7.4, 154 mm NaCl) and non-physiological (pH 3.0, 5.0, 6.5, and 7.4) conditions to examine the release mechanism. After the loading procedure, the ChMAP-28-loaded silk particles were collected via centrifugation and redispersed in the corresponding release medium. To investigate release kinetics, the supernatant in the release medium was obtained by centrifugation at different time points and analyzed for total protein content using the BCA Protein Assay Kit, as described above. Each release experiment was conducted in triplicate over 30 days. The timepoints for drug release measurements were 1, 2, 4, 6, 8, 10, 12, 15, 17, 20, 22, 25, 30 d of incubation.

Flow Cytometry

Flow cytometry was performed on a NovoCyte flow cytometer (ACEA Biosciences). Cell death analysis with annexin V-FITC/propidium iodide (PI) double staining was conducted 4 h after the addition of ChMAP-28-loaded particles, up to a final concentration of 5 μM. The Each experiment was performed in triplicates.

Statistics

The statistical significance of the differences between groups was evaluated using analysis of variance (ANOVA) by GraphPad prism. Post hoc tests with the Bonferroni correction were performed. Differences between groups were considered significant when the *p*-value was less than 0.01.

Results and Discussions

Preparation and Colloidal Stability of M4R2, M4R4, and M4R6 Particles

To investigate the effect of molecular weight on the properties of the silk particles, we expressed and purified three recombinant silk proteins: M4R2, M4R4, and M4R6. M4R2, M4R4, and M4R6 possess different numbers of repeat units (2 for M4R2, 4 for M4R4, and 6 for M4R6), which are derived from the spider silk protein MaSp4 of *A. ventricosus*.[23] Despite their distinct molecular weights, all three proteins share the same isoelectric point (5.5) and hydrophilic value (−0.77). Unlike other MaSp proteins, the repetitive region of MaSp4 lacks the poly alanine motifs typical of MaSp1 and MaSp2 but is rich in the unique motif GPGPQ that forms β-turns.[22,23] The His_6-tag was added to the C-terminus to facilitate purification. The average yields of purified proteins for M4R2, M4R4, and M4R6 were approximately 30, 20, and 10 mg/L, respectively. SDS-PAGE analysis showed that the purity of the recombinant proteins was >90%, and that they exhibited migration patterns similar to the predicted molecular masses (Figure 1B).

Spider silk particles were produced using the salting-out method through rapid mixing with a high molar concentration of potassium phosphate buffer, which has been widely utilized for the production of nanoparticles from bioengineered spider silk.[16,24–26] The preparation of M4R2, M4R4, and M4R6 particles using the salting-out method resulted in particle sizes of 122 ± 12 nm, 131 ± 10 nm, and 122 ± 9 nm, respectively, as confirmed by scanning electron microscopy. (Figure 2A and B). Furthermore, the colloidal stability of silk particles in potassium phosphate solution was analyzed at different pH values (7, 6.5, and 6) and ionic strengths (50, 100, and 154 mm NaCl). We found that all three particles were colloidally stable at pH 7, 6.5, and ultrapure water over a period of 24 h, whereas a decrease in pH towards (pH 6) the isoelectric point (pI) of proteins led to significant particle agglomeration (Figure 2C). Conversely, at pH 6, all three spider silk particles demonstrated instability at all ionic strengths and presented agglomeration, which might be explained by the effect of ionic strength on zeta potential (Figure 2D). In addition, agglomeration of the M4R6 particles was more pronounced than that of the M4R2 and M4R4 particles, which may be due to their higher molecular weights (Figure 2D). To further determine whether ionic strength strongly influences the zeta potential of the charged particles, the zeta potentials of these three particles at different pH and ionic strengths were analyzed. The results demonstrated that the zeta

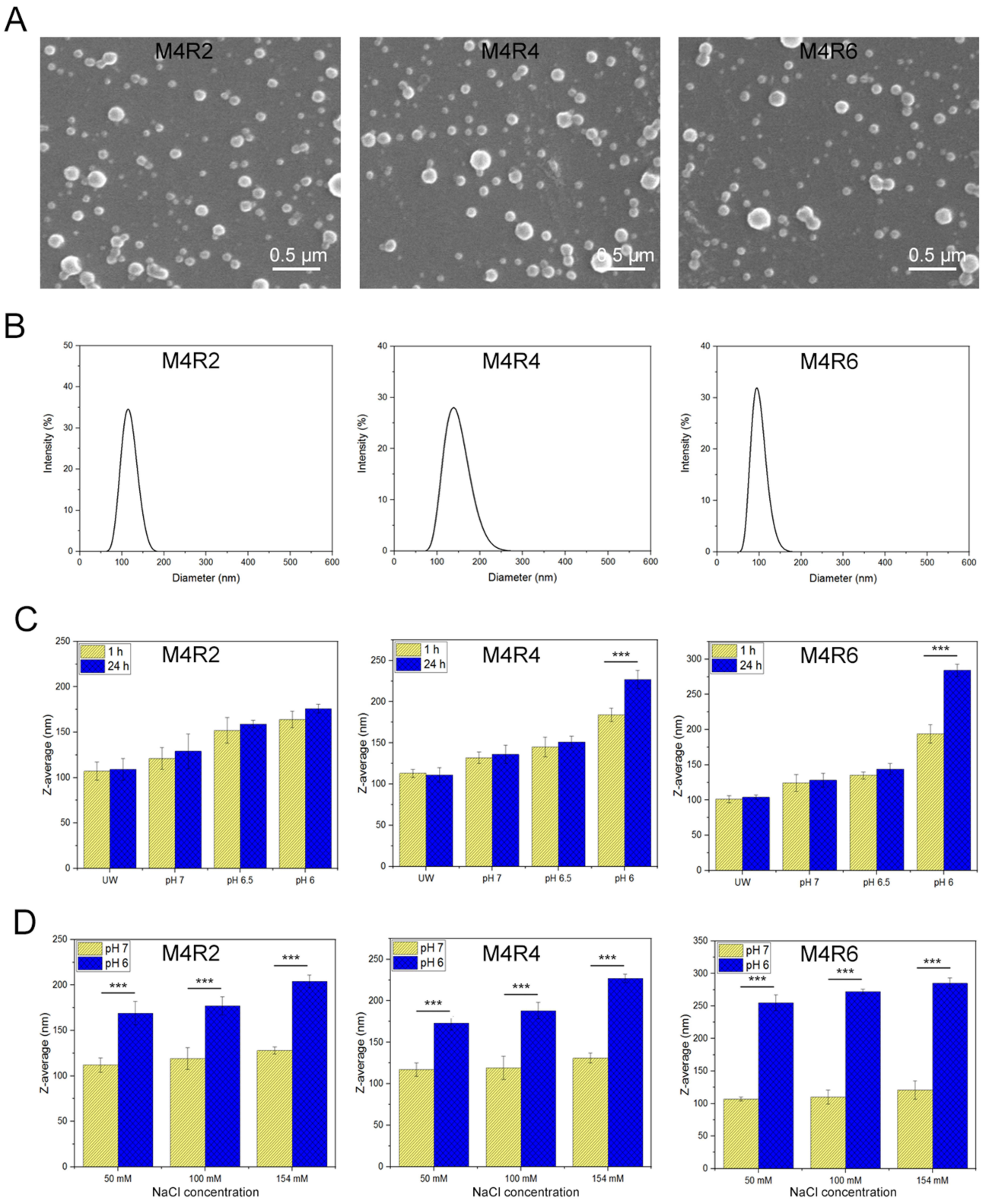

Figure 2 Size and morphological analysis of the M4R2, M4R4, and M4R6 particles. (**A**) SEM micrograph of the M4R2, M4R4, and M4R6 particles. (**B**) Particle size distribution of the M4R2, M4R4, and M4R6 particles. (**C**) Particle size of M4R2, M4R4, and M4R6 particles after 1 h and 24 h storage at 10 mm phosphate buffer with varying pH values (pH 7, 6.5, and 6). Ultrapure water is indicated by UW. (**D**) Particle size of M4R2, M4R4, and M4R6 particles incubated for 24 h at pH 7 and 6 at different ionic strengths (50 mm, 100 mm, 154 mm NaCl). A Student's *t*-test was used to evaluate statistical significance (***p<0.001).

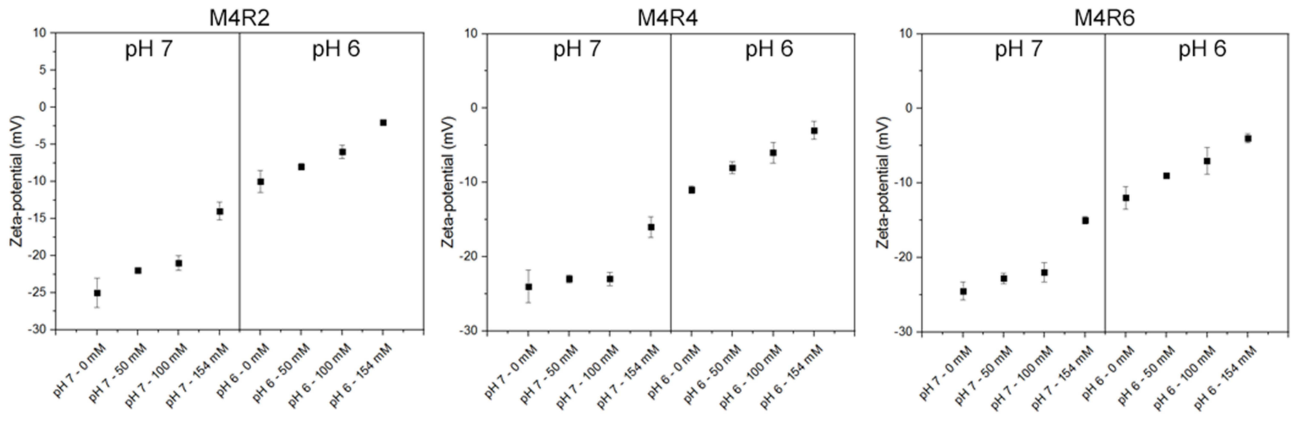

Figure 3 Zeta-potential of M4R2, M4R4, and M4R6 particles at different pH and NaCl concentration.

potential values for the M4R2, M4R4, and M4R6 particles decreased from approximately −25 mV at pH 7 without NaCl to lower than −5 mV at pH 6 and an ionic strength of 154 mm (Figure 3). Given the pI value of 5.5 for these three proteins, the reduction of particle charge led to the weakening of the electrostatic repulsive force between particles when the pH value decreased from 7 to 6 (close to pI). Moreover, the increase in ionic strength can reduce the charge of the silk particles to a certain extent, thereby contributing to their aggregation.[27] Nevertheless, the reduction in particle charge caused by high ionic strength can effectively promote drug release under physiological conditions (pH 7.4, 154 mm NaCl).[20] To evaluate the long-term stability of M4R2, M4R4, and M4R6 particles in ultrapure water, the particle size was monitored at 4°C over a period of three months, and exhibited colloidal stability during storage. In addition, the particle size was also stable under physiological conditions (pH 7.4, 37°C) over one month. These results demonstrate that the M4R2, M4R4, and M4R6 particles are colloidally stable in neutral solutions without ionic strength.

Cytotoxicity

There is no doubt that the biocompatibility of medical biomaterials must be guaranteed,[28–30] the cytotoxicity of these three particles was investigated. The cytotoxicity study showed that M4R2, M4R4, and M4R6 particles were not toxic, and a slight decrease in cell viability was observed at the highest particle concentrations, similar to other MaSp-based silk particles (Figure 4).[18,31–34] Furthermore, the differences between different particle types were not significant.

Loading of Silk Particles With ChMAP-28

All three silk particles exhibited an overall negative charge in ultrapure water and potassium phosphate buffer with a pH of 6 or higher, owing to their pI value of 5.5 (Figure 3). Previous studies have shown that recombinant spider silk particles can be loaded with positively charged molecular drugs of low molecular weight.[16] To evaluate the possibility of loading these three silk particles with peptide drugs, the antitumor peptide ChMAP-28 was chosen as a peptide compound with an isoelectric point of 12 kDa and molecular weight of 3.3 kDa.[35] Owing to its high pI value, ChMAP-28 exhibits a positive net charge at pH 7.

The results showed that ChMAP-28 was loaded onto all three silk particles in large quantities (Figure 5A). It was possible to load more than 40% (w/w) of ChMAP-28 by simple incubation of M4R2, M4R4, and M4R6 particles in ChMAP-28 containing phosphate buffer (pH 7) without NaCl. Given the relatively low zeta-potential of these silk proteins, the electrostatic interaction strength between particles and ChMAP-28 may be insufficient to achieve higher drug loading. Therefore, genetic modifications that introduce negatively charged amino acid residues to further decrease protein pI could enhance the loading capacity. Although the loading efficiencies of these three silk particles declined with increasing w/w ratio, the associated loading efficiency for M4R2 particles remained above 90% for w/w ratios ranging from 2.5% to 30%, which was significantly higher than that of the other two particles, indicating a highly effective loading of ChMAP-28 for M4R2 particles (Figure 5A). Moreover, the influence of ionic strength on the loading and loading efficiencies of the three silk particles was analyzed. An increase in NaCl concentration from 50 to 100 mm led to

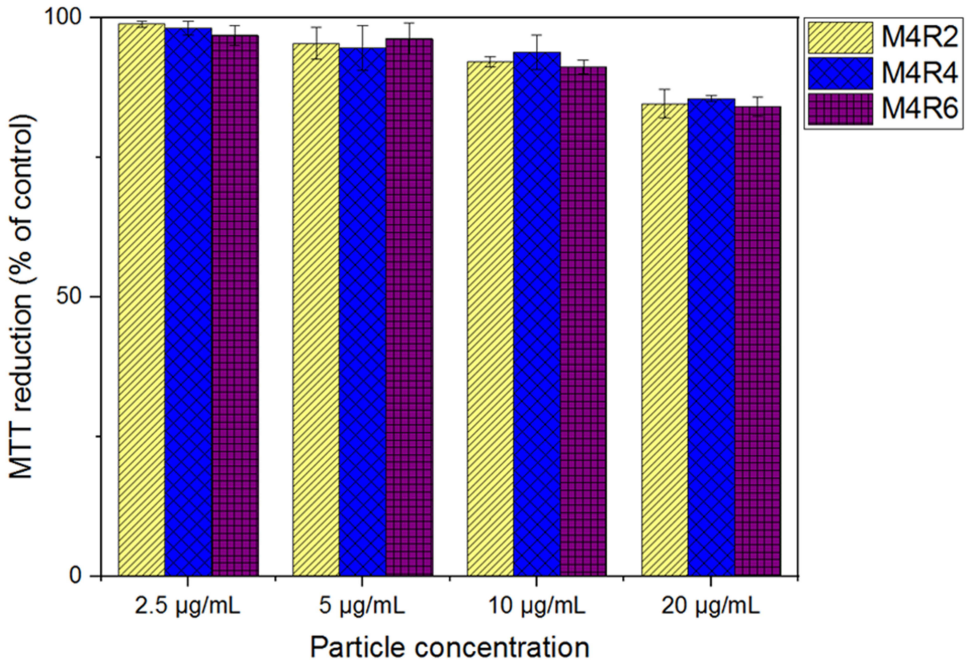

Figure 4 Cytotoxicity study of M4R2, M4R4, and M4R6 particles by MTT assay.

a distinct decrease in the loading and loading efficiencies (Figure 5B and C). For the M4R2 particles, the loading at 60% w/w ratio decreased from 46% in phosphate buffer (pH 7) without NaCl to 37% in phosphate buffer (pH 7) with 100 mm NaCl. Meanwhile, the loading efficiency at a w/w ratio of 60% was reduced from 67 to 48% (Figure 5B and C). For M4R4 particles, the loading at a 60% w/w ratio was reduced from 41% in phosphate buffer (pH 7) without NaCl to 34% in phosphate buffer (pH 7) with 100 mm NaCl. Furthermore, the loading efficiency of M4R4 particles at a w/w ratio of 60% was reduced from 64 to 43% (Figure 5B and C). For the M4R6 particles, the loading at a 60% w/w ratio was reduced from 40% in phosphate buffer (pH 7) without NaCl to 31% in phosphate buffer (pH 7) with 100 mm NaCl, and the loading efficiency of the M4R6 particles at a 60% w/w ratio was reduced from 58% to 42% (Figure 5B and C). These results clearly suggest that the loading of negatively charged M4R2, M4R4, and M4R6 particles with positively charged ChMAP-28 is mainly driven by electrostatic interactions.

In vitro Release of ChMAP-28 From Silk Particles

The in vitro release of ChMAP-28 from M4R2, M4R4, and M4R6 particles was investigated in phosphate buffers with different pH and ionic strengths. At pH 3 and 4, almost 80% and 60% of ChMAP-28 was released from the M4R2 particles within the first 24 h (Figure 6A). Furthermore, nearly 100% of ChMAP-28 was released from the M4R2 particles after 12 days (Figure 6A). In contrast, although ChMAP-28 was released from the other two particles more rapidly, only 90% of the ChMAP-28 was released from the M4R4 and M4R6 particles after 12 days (Figure 6A). In addition, no significant amounts of ChMAP-28 were detected for the three silk particles at pH 7.4 and pH 6.5 even after 30 days, indicating the existence of very strong electrostatic interactions between recombinant proteins and ChMAP-28 at these two pH levels. In contrast, the release profiles indicated that reducing the ionic strength from 154 mm to ultrapure water led to a substantial decrease in the released ChMAP-28 for the three particles from 37% to nearly undetectable amounts after 30 d of incubation (Figure 6B). In addition, the release of ChMAP-28 from M4R4 and M4R6 particles was faster than that from M4R2 particles, indicating that M4R2 particles can be used as drug sustained-release carriers for positively charged peptide drugs (Figure 6B). To investigate the relation between particle size and release behavior, in vitro release of drug from silk particles with different PI and averaged size was analyzed over a week (Figure 6C and D). Within the first 24 hours, all silk particle types exhibited an initial burst release, followed by a steady-state drug release. This burst release was beneficial for suppressing cancer cell replication within a short period of time.

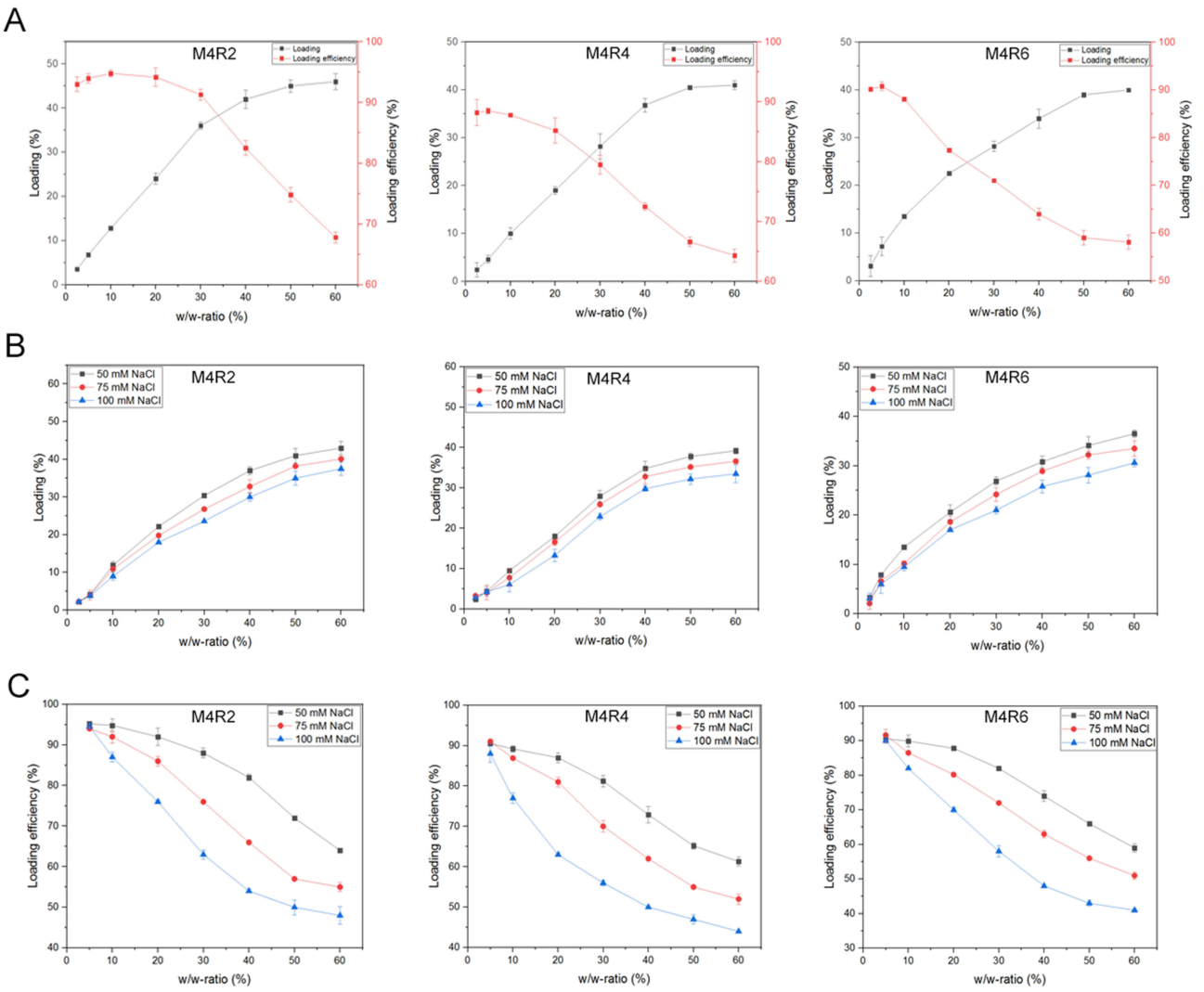

Figure 5 Loading of M4R2, M4R4, and M4R6 particles with ChMAP-28. (**A**) Loading and loading efficiencies of the w/w-ratio of ChMAP-28-loaded silk particles in the incubation buffer at 10 mm phosphate buffer (pH 7, 20 mm NaCl). (**B**) Loading of silk particles with ChMAP-28 at 10 mm phosphate buffer (pH 7) with different NaCl concentrations. (**C**) Loading efficiencies of ChMAP-28 at 10 mm phosphate buffer (pH 7) with different NaCl concentrations.

Additionally, for silk particles of the same type, those with larger size and polydispersity index (PI) released the drug slightly more slowly compared to smaller particles with lower PI (Figure 6C and D). The result showed that ChMAP-28-loaded silk particles readily penetrated tumor cells (Figure 7). Based on these results, it can be concluded that the release of ChMAP-28 from silk particles was predominantly controlled by the degree of electrostatic interaction. Specifically, a decrease in pH and an increase in ionic strength weakened the electrostatic interactions between positively charged ChMAP-28 and negatively charged M4R2, M4R4, and M4R6 particles, such that ChMAP-28 was released from the particles at low pH (< 4) or high ionic strength (154 mm), whereas ChMAP-28 sticked to the particles under neutral conditions and low ionic strength. Recently, Han et al demonstrated that particles composed of recombinant silk protein rAcSp2 exhibited stability and efficiently bound peptide drugs via electrostatic interactions; however, they also exhibited a rapid release rate within 10 days.[36] By contrast, M4R2 particles not only display high loading efficiency, but also have better sustained release properties. Due to the limitations of the singularly designed recombinant protein, it is challenging to identify a promising candidate that possesses both high loading efficiency and excellent sustained-release properties. Therefore, our three designed recombinant silk proteins, which vary in molecular weight and material properties, enable the selection of a more ideal drug carrier.

https://doi.org/10.2147/IJN.S510273

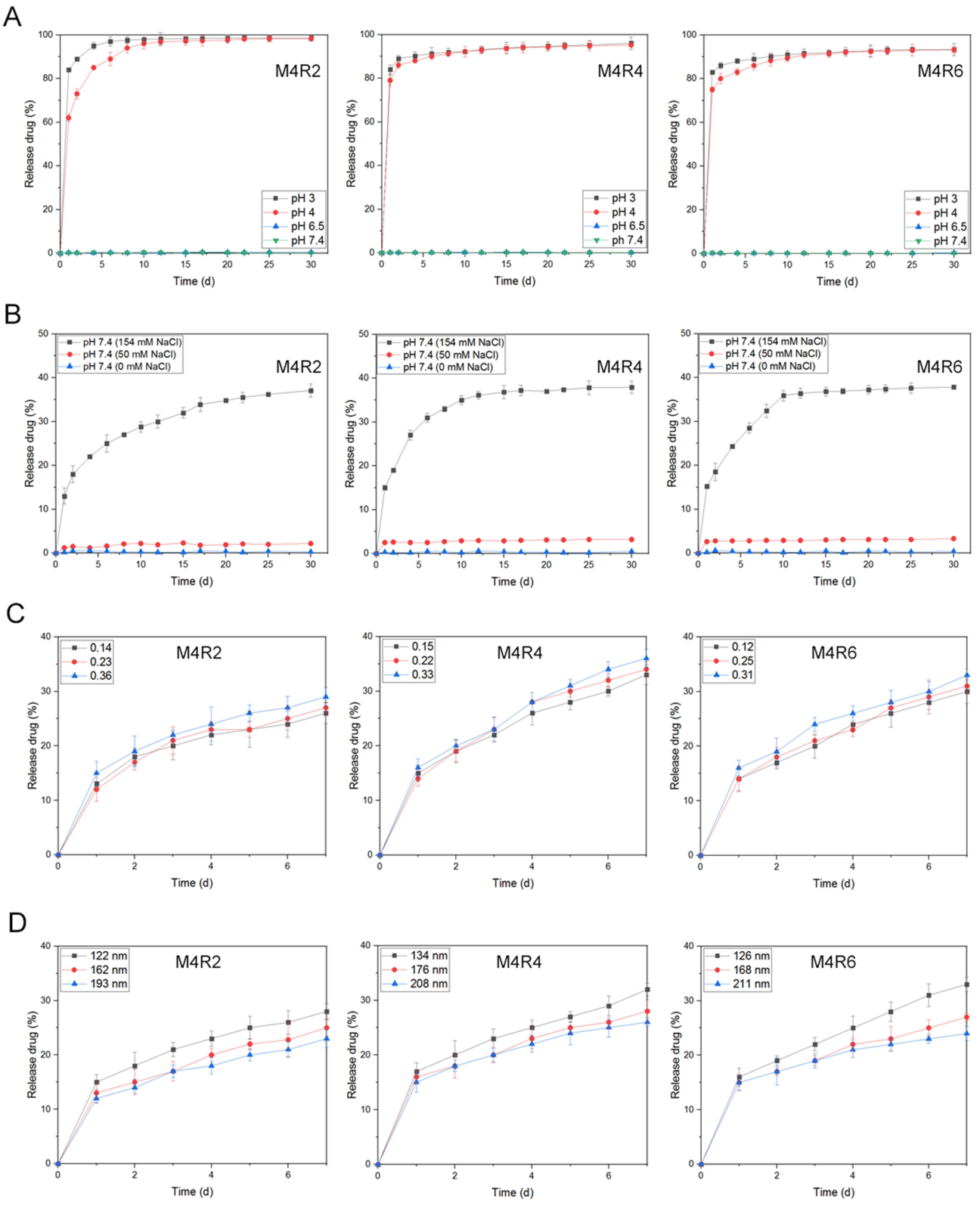

Figure 6 In vitro release of ChMAP-28 from silk particles. (**A**) Influence of pH on the in vitro release of ChMAP-28 from silk particles over 30 days. (**B**) Influence of ionic strength on the in vitro release from ChMAP-28-loaded silk particles at pH 7.4 over 30 days. (**C**) Influence of PI on the in vitro release of ChMAP-28 from silk particles over a week. (**D**) Influence of averaged particle size on the in vitro release of ChMAP-28 from silk particles over a week.

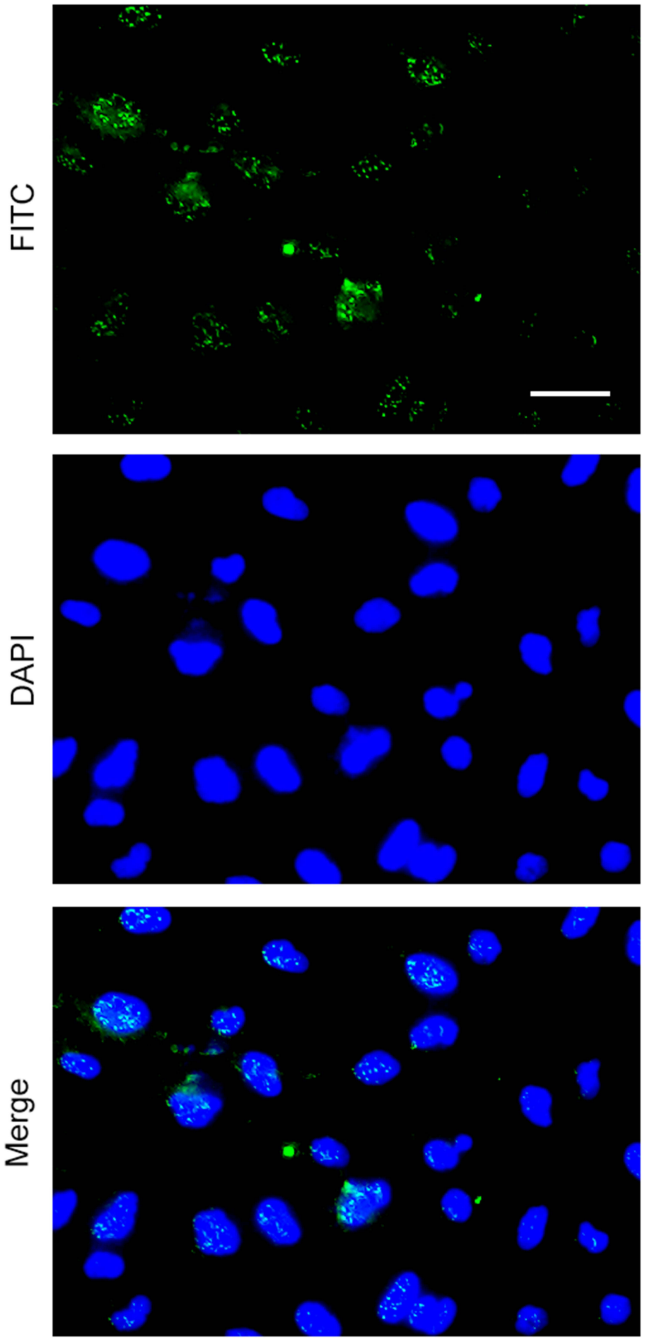

Figure 7 Confocal microscopy analysis of H1299 cells when incubated with M4R2 particles loaded with ChMAP-28-FITC for 4 h. Scale bar: 20 μm.

The Proapoptosis Effect of ChMAP-28-Loaded M4R2 Particles

A previous study has shown that ChMAP-28 can induce apoptosis in tumor cells. H1299 cells were treated with ChMAP-28-loaded M4R2 particles for 48 h and analyzed by flow cytometry (Figure 8); the results are shown in Figure 8. The apoptosis rate of the M4R2 particle group was almost equal to that of the control group, indicating excellent biocompatibility, which is consistent with the cell viability results (Figure 8). In contrast, treatment with ChMAP-28-loaded M4R2 particles resulted in an apoptosis rate of 86% in H1299 cells, which was significantly higher than that in the M4R2 particle group, suggesting that ChMAP-28-loaded M4R2 particles can induce apoptosis in tumor cells.

https://doi.org/10.2147/IJN.S510273

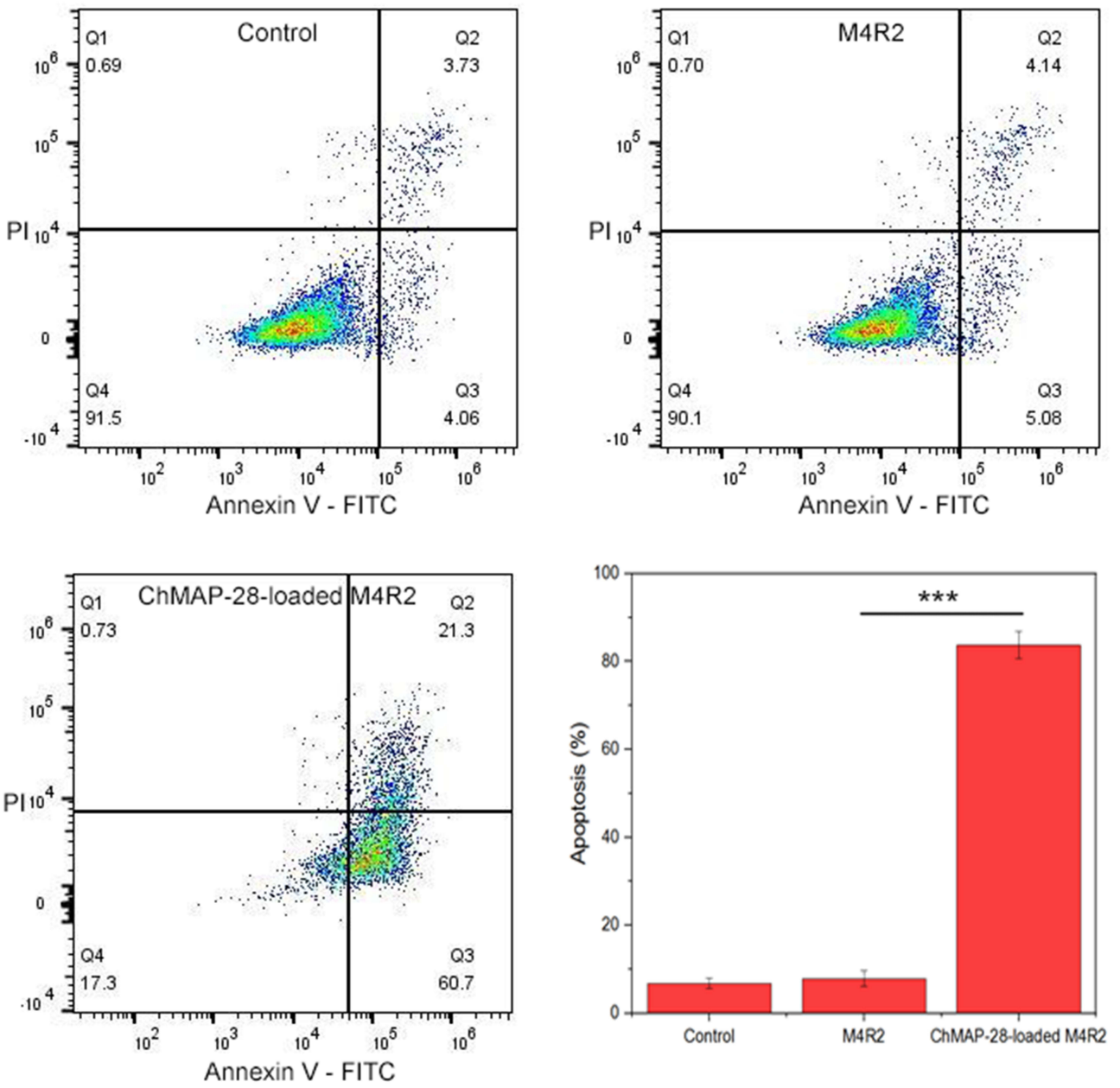

Figure 8 Cytotoxicity of ChMAP-28 and ChMAP-28-loaded M4R2 particles for human non-small cell lung cancer cells (H1299) was assessed by flow cytometry. A Student's *t*-test was used to evaluate statistical significance (***p<0.001).

Conclusions

In this study, we designed three new variants of recombinant silk proteins, M4R2, M4R4, and M4R6. M4R2, M4R4, and M4R6 were constructed based on the sequences of different numbers of repeat units from *A. ventricosus* MaSp4. We obtained particles with characteristics different from those of the three recombinant proteins. Despite very similar particle sizes under neutral pH, low ionic strength, and ultrapure water, the M4R4 and M4R6 particles exhibited a higher tendency to aggregate at acidic pH and high ionic strength than the M4R2 particles. Moreover, large quantities of ChMAP-28 were loaded onto these three particles with at least 90% loading efficiency because of the strong electrostatic interactions between the positively charged ChMAP-28 and negatively charged M4R2, M4R4, and M4R6 particles. Under neutral conditions (in the absence of ions), positively charged drugs are loaded onto negatively charged silk particles. However, under conditions of high ionic strength, such as physiological conditions (pH 7.4, 154 mm NaCl), the

electrostatic interactions between the drugs and silk particles are weakened, leading to drug release from the particles. A faster release rate of ChMAP-28 from M4R4 and M4R6 particles than from M4R2 particles was also observed. Similar to other recombinant silk proteins, our three combined silk proteins were not cytotoxic. M4R2 particles exhibit superior performance in colloidal stability and drug loading efficiency compared to other biopolymer-based drug carriers, such as chitosan and gelatin nanoparticles, demonstrating lower aggregation tendencies and higher drug loading efficiency under acidic pH and high ionic strength conditions.[37] Additionally, M4R2 provides more controlled drug release rates under neutral conditions, outperforming PLGA nanoparticles.[38] In our future work, we will further conduct comprehensive in vivo studies to evaluate biodistribution, pharmacokinetics, and therapeutic efficacy, thereby ensuring the feasibility and effectiveness of this system for biomedical applications. In conclusion, the combination of strong colloidal stability, high loading efficiency, and favorable release rate makes M4R2 particles the most suitable for delivering peptide drug molecules with a positive charge.

Acknowledgment

This study was supported by the China Postdoctoral Science Foundation (grant number: 2021M703165).

Disclosure

The authors report no conflicts of interest in this work.

References

1. Birk SE, Boisen A, Nielsen LH. Polymeric nano- and microparticulate drug delivery systems for treatment of biofilms. *Adv. Drug Deliv Rev.* 2021;174:30–52. doi:10.1016/j.addr.2021.04.005
2. Liang Q, Cheng Z, Qin L. Advanced nanoparticles in osteoarthritis treatment. *Biomater Transl*. 2024;5(2):95–113. doi:10.12336/biomatertransl.2024.02.002
3. Lamboni L, Gauthier M, Yang G, Wang Q. Silk sericin: a versatile material for tissue engineering and drug delivery. *Biotechnol Adv*. 2015;33(8):1855–1867. doi:10.1016/j.biotechadv.2015.10.014
4. Gombotz WR, Pettit DK. Biodegradable polymers for protein and peptide drug delivery. *Bioconjug Chem*. 1995;6(4):332–351. doi:10.1021/bc00034a002
5. Wenk E, Merkle HP, Meinel L. Silk fibroin as a vehicle for drug delivery applications. *J Control Release*. 2011;150(2):128–141. doi:10.1016/j.jconrel.2010.11.007
6. Wilar G, Suhandi C, Wathoni N, Fukunaga K, Kawahata I. Nanoparticle-Based Drug Delivery Systems Enhance Treatment of Cognitive Defects. *Int J Nanomed*. 2024;19:11357–11378. doi:10.2147/IJN.S484838
7. Su Y, Zhang B, Sun R, et al. PLGA-based biodegradable microspheres in drug delivery: recent advances in research and application. *Drug Deliv.* 2021;28(1):1397–1418. doi:10.1080/10717544.2021.1938756
8. Yang J, Zeng H, Luo Y, et al. Recent Applications of PLGA in Drug Delivery Systems. *Polymer*. 2024;16(18):2606. doi:10.3390/polym16182606
9. van de Weert M, Hennink WE, Jiskoot W. Protein instability in poly(lactic-co-glycolic acid) microparticles. *Pharm Res*. 2000;17(10):1159–1167. doi:10.1023/A:1026498209874
10. Brunner A, Mäder K, Göpferich A. pH and osmotic pressure inside biodegradable microspheres during erosion. *Pharm Res*. 1999;16(6):847–853. doi:10.1023/A:1018822002353
11. Cui L, Perini G, Minopoli A, et al. Plant-derived extracellular vesicles release combined with systemic DOX exhibits synergistic effects in 3D bioprinted triple-negative breast cancer. *Biomed Pharmacother*. 2024;181:117637. doi:10.1016/j.biopha.2024.117637
12. Mendes GG, Faulk B, Kaparthi B, et al. Genetic Functionalization of Protein-Based Biomaterials via Protein Fusions. *Biomacromolecules*. 2024;25(8):4639–4662. doi:10.1021/acs.biomac.4c00188
13. Numata K, Kaplan DL. Silk-based delivery systems of bioactive molecules. *Adv Drug Deliv Rev*. 2010;62(15):1497–1508. doi:10.1016/j.addr.2010.03.009
14. Debabov VG, Bogush VG. Recombinant Spidroins as the Basis for New Materials. *ACS Biomater Sci Eng*. 2020;6(7):3745–3761. doi:10.1021/acsbiomaterials.0c00109
15. Schacht K, Scheibel T. Processing of recombinant spider silk proteins into tailor-made materials for biomaterials applications. *Curr Opin Biotechnol*. 2014;29:62–69. doi:10.1016/j.copbio.2014.02.015
16. Lammel A, Schwab M, Hofer M, Winter G, Scheibel T. Recombinant spider silk particles as drug delivery vehicles. *Biomaterials*. 2011;32(8):2233–2240. doi:10.1016/j.biomaterials.2010.11.060
17. Hofer M, Winter G, Myschik J. Recombinant spider silk particles for controlled delivery of protein drugs. *Biomaterials*. 2012;33(5):1554–1562. doi:10.1016/j.biomaterials.2011.10.053
18. Kucharczyk K, Weiss M, Jastrzebska K, et al. Bioengineering the spider silk sequence to modify its affinity for drugs. *Int J Nanomed*. 2018;13:4247–4261. doi:10.2147/IJN.S168081
19. Florczak A, Jastrzebska K, Mackiewicz A, Dams-Kozlowska H. Blending two bioengineered spider silks to develop cancer targeting spheres. *J Mater Chem B*. 2017;5(16):3000–3011. doi:10.1039/C7TB00233E
20. Jastrzebska K, Florczak A, Kucharczyk K, et al. Delivery of chemotherapeutics using spheres made of bioengineered spider silks derived from MaSp1 and MaSp2 proteins. *Nanomedicine*. 2018;13(4):439–454. doi:10.2217/nnm-2017-0276

21. Garb JE, Haney RA, Schwager EE, et al. The transcriptome of Darwin's bark spider silk glands predicts proteins contributing to dragline silk toughness. *Commun Biol*. 2019;2(1):275. doi:10.1038/s42003-019-0496-1
22. Kono N, Nakamura H, Ohtoshi R, et al. Orb-weaving spider *Araneus ventricosus* genome elucidates the spidroin gene catalogue. *Sci Rep*. 2019;9 (1):8380. doi:10.1038/s41598-019-44775-2
23. Wen R, Wang S, Wang K, Yang D, Zan X, Meng Q. Complete gene sequence and mechanical property of the fourth type of major ampullate silk protein. *Acta Biomater*. 2023;155:282–291. doi:10.1016/j.actbio.2022.11.042
24. Florczak A, Mackiewicz A, Dams-Kozlowska H. Functionalized spider silk spheres as drug carriers for targeted cancer therapy. *Biomacromolecules*. 2014;15(8):2971–2981. doi:10.1021/bm500591p
25. Kucharczyk K, Florczak A, Kaminska A, et al. MMPs-responsive silk spheres for controlled drug release within tumor microenvironment. *Int J Biol Macromol*. 2024;269(Pt 1):132016. doi:10.1016/j.ijbiomac.2024.132016
26. Jastrzebska K, Felcyn E, Kozak M, et al. The method of purifying bioengineered spider silk determines the silk sphere properties. *Sci Rep*. 2016;6 (1):28106. doi:10.1038/srep28106
27. Doblhofer E, Scheibel T. Engineering of recombinant spider silk proteins allows defined uptake and release of substances. *J Pharm Sci*. 2015;104 (3):988–994. doi:10.1002/jps.24300
28. Lewicka M, Hermanson O, Rising AU. Recombinant spider silk matrices for neural stem cell cultures. *Biomaterials*. 2012;33(31):7712–7717. doi:10.1016/j.biomaterials.2012.07.021
29. Branković M, Zivic F, Grujovic N, Stojadinovic I, Milenkovic S, Kotorcevic N. Review of Spider Silk Applications in Biomedical and Tissue Engineering. *Biomimetics*. 2024;9(3):169. doi:10.3390/biomimetics9030169
30. Allmeling C, Jokuszies A, Reimers K, et al. Spider silk fibres in artificial nerve constructs promote peripheral nerve regeneration. *Cell Prolif*. 2008;41(3):408–420. doi:10.1111/j.1365-2184.2008.00534.x
31. Dams-Kozlowska H, Majer A, Tomasiewicz P, Lozinska J, Kaplan DL, Mackiewicz A. Purification and cytotoxicity of tag-free bioengineered spider silk proteins. *J Biomed Mater Res A*. 2013;101(2):456–464. doi:10.1002/jbm.a.34353
32. Zhang C, Mi J, Qi H, et al. Engineered a novel pH-sensitive short major ampullate spidroin. *Int J Biol Macromol*. 2020;154:698–705. doi:10.1016/j.ijbiomac.2020.03.153
33. Deptuch T, Penderecka K, Kaczmarek M, Molenda S, Dams-Kozlowska H. In vivo study of the immune response to bioengineered spider silk spheres. *Sci Rep*. 2022;12(1):13480. doi:10.1038/s41598-022-17637-7
34. Deptuch T, Florczak A, Lewandowska A, et al. MS1-type bioengineered spider silk nanoparticles do not exhibit toxicity in an *in vivo* mouse model. *Nanomedicine*. 2021;16(18):1553–1565. doi:10.2217/nnm-2021-0029
35. Emelianova AA, Kuzmin DV, Panteleev PV, Sorokin M, Buzdin AA, Ovchinnikova TV. Anticancer Activity of the Goat Antimicrobial Peptide ChMAP-28. *Front Pharmacol*. 2018;9:1501. doi:10.3389/fphar.2018.01501
36. Han F, Li X, Tan Y, Zhou Q. Particles made of a novel recombinant spider silk protein rAcSp2 as delivery system for peptide drugs with anti-tumor activity. *BIOCHEM ENG J*. 2025;214:109588. doi:10.1016/j.bej.2024.109588
37. Zhang Q, Liang J, Yun SLJ, Liang K, Yang D, Gu Z. Recent advances in improving tumor-targeted delivery of imaging nanoprobes. *Biomater Sci*. 2020;8(15):4129–4146. doi:10.1039/D0BM00761G
38. Wang H, Li J, Wang Y, et al. Nanoparticles-mediated reoxygenation strategy relieves tumor hypoxia for enhanced cancer therapy. *J Control Release*. 2020;319:25–45. doi:10.1016/j.jconrel.2019.12.028